International Journal of Scientific Engineering and Research (IJSER)
ISSN (Online): 2347-3878
Index Copernicus Value (2015): 56.67 | Impact Factor (2017): 5.156

Discrete Element Simulation of Granular Particles in a Rotating Cylinder

Oleena S. H.[1]

Kerala University Library, Palayam, Thiruvananthapuram, Kerala, India
oleenaroy[at]gmail.com

Abstract: ***The objective of this contribution is to present a numerical simulation method to model the motion of a packed bed on a moving grate or in a rotary kiln using object-oriented techniques. The packed bed can be described as granular material consisting of a large number of particles. The method chosen is the Lagrangian time-driven method and it uses the position, the orientation, the velocity and the angular velocity of particles as independent variables. These are obtained by time integration of the three-dimensional dynamics equations which were derived from the classical Newtonian mechanics approach based on the second law of Newton for the translation and rotation of each particle in the granular material. This includes keeping track of all forces and moments acting on each particle at every time-step. Particles are treated as contacting visco-elastic bodies which can overlap each other. Contact forces depend on the overlap geometry, material properties and dynamics of particles and include normal and tangential components of repulsion force with visco-elastic models for energy dissipation through internal and surface friction. The resulting equations of particle motion are solved by the Gear predictor–corrector scheme of fifth-order accuracy. A discrete element method (DEM) study is conducted to investigate the mixing characteristics of spherical particles and flow regimes of a rotating tumbler. The back ground version of DEM and time integration algorithm are developed and implemented into C++ code. The implementation of time-integration algorithm is verified by simple test concerning particle-particle, particle-wall interaction for which analytical expression exist. In this paper particle force due to different material property are investigated.***

Keywords: DEM simulation, Granular materials.

1. Introduction

Rotating Cylinder play a noticeable role in the processing of granular material in chemical industries in an extensive variety of physical processes, including size reduction, waste reclamation, agglomeration, solid mixing, drying, heating, cooling, etc. The general use of rotating cylinder is also caused by its ability to handle various feedstock, from slurries to granular materials, and to activate in distinct environments. Rotary cylinders are the most usually used mixing devices in metallurgical and catalyst industries. Rotary dryers play an important role in many industrial applications, such as chemistry, metallurgy and materials science, mineral industries, and food processing (O.O. Ajayi [2012], P. Shao et, al [2015]). It is important to recognize the mixing characteristics and heat transfer presentation. DEM models are the study of mixing in various amalgamation systems including rotating drum (Chaudhuri et al., 2006). Particle transport is vital and happens in two directions: transverse and axial. Particle transport in the transverse direction is comparatively uniform, while particle transport in the axial direction may diverge with different residence time.

The discrete element method (DEM), originally developed by (Cundall (1971) and Cundall and Strack (1979)), has been used successfully to simulate chute flow (Dippel et al., 1996), heap formation (Luding, 1997), hopper discharge (Thompson and Grest, 1991; Ristow and Herrmann, 1994), blender segregation (Wightman et al., 1998; Shinbrot et al., 1999; Moakher et al., 2000) and flows in rotating drums (Ristow, 1996; Wightman et al., 1998).

The DEM allows for the simulation of particle motion and interaction between the particles, taking into account not only the obvious geometric and material effects such as particle shape, material non-linearity, viscosity, friction, etc, but also the effect of various physical fields of surrounding media, even of chemical reactions (Kantor et al. 2000)Recently, DEM has been used for the solution of discrete and continuous problems including solid, fluid and molecular mechanics, heat transfer etc (Tanska et al. 2002, Kantor et al. 2000, Kuwagia et al. 2002, Cleary et al. 2002**,** Li et al. 2000, Tran et al. 1998, Peters et al, 2001).

One of the most promising area of future applications of discrete element method seems to be geotechnical engineering. The discrete approach assumes the soil is an assembly of granules or discrete particles where micromechanical behavior of soil is pre-defined by micromechanical inter granular properties.

2. Discrete State Formulation

The granular media present a space filled by the particle termed here as discrete elements. The media are assumed to be composed of spherical particles with same radii R_i. The particles are assumed to be deformable bodies, deforming each other by normal and shear force.

The composition of media is time-dependent because distinct particle change their position by free rigid body motion or by contacting with neighbor particles or walls. Each particle may be in contact with other particles.

The visco-elastic material of granular media is defined by the modulus of elasticity, Poisson's ratio and damping coefficients in normal and shear directions. The boundary conditions of media are determined by planes and treated as particles with an infinite radius and mass. The external is induced with kinematic boundary conditions which are implemented by the walls movements.

The dynamic behaviour of media is considered as the dynamics of each particle. Consequently, the overall response of media is predicted by the behaviour of individual particles, the dynamics of which is evaluated by applying the second Newton's law. One of the most important issues considered by a discrete approach is the detection of interaction force between contacting particles. The interaction forces of each contacting pair are locally resolved on the basis of actual geometry of kinematic contact between two spherical particles, inter-particle contact forces and boundary conditions.

3. Geometry of Kinematic Contact of Spherical Particles

Let any two particles i and j be in contact with position vectors x_i and x_j with center of gravity lying at O_i and O_j having linear velocities v_i and v_j, angular velocities ω_i and ω_j respectively (Algis Dzingys [2001]).

The contact point c_{ij} is defined to be at the center of the overlap area position vector x_{cij} .The vector x_{ij} of the relative position point from the center to gravity of particle i to that of particle j is defined as $x_{ij} = x - x_j$. The depth of overlap is h_{ij}. Unit vector in the normal direction of the contact surface through the center of the overlap area is denoted by n_{ij}. It extends from the contact point to the inside of the particle i as $n_{ij} = n_{ji}$

The vector d_{cij} and d_{cji} are directed towards the contact point from the centers of particle i and particle j respectively and are represented as

$$d_{cij} = x_{cij} - x_i$$
$$d_{cji} = x_{cji} - x_j$$

Since the particle shape is assumed to be spherical, for sphere of any dimension the contact parameters can be written as follows:

$$h_{ij} = \begin{cases} R_i + R_j - |x_{ij}|, |x_{ij}| < R_i + R_j \\ 0, |x_{ij}| \geq R_i + R_j \end{cases}$$

$$d_{cij} = -\left(R_i - \frac{h_{ij}}{2}\right) n_{ij}$$

Where R is the radius of the particle. The relative velocity of the contact point is defined as

$$v_{ij} = v_{cij} - v_{cji}$$

where

$$v_{cij} = v_i + \omega_i \times d_{cij}$$
$$v_{cji} = v_j + \omega_j \times d_{cji}$$

are the velocities of particle i and particle j respectively. The normal and tangential component of the relative velocities are defined by

$$v_{n,ji} = (v_{ij} \cdot n_{ij}) n_{ij}$$

and

$$v_{t,ji} = v_{ij} - v_{n,ij}$$

In case of contact with partial slip, particles may slip relative to the distance

$\delta_{t,ij}$ is the integrated slip in tangential direction after particles i and j came into contact and can be defined by the equation,

$$\delta_{t,ij} = \left| \int v_{t,ij}(t) dt \right|$$

Here $\delta_{t,ij}$ is allowed to increase until the tangential force exceeds the limit imposed by static friction. The vector of tangential displacement $\delta_{t,ij}$ is defined to be perpendicular to the normal contact direction and located on the same line as $v_{t,ij}$. If the tangential component of the contact velocity $v_{t,ij}$ is not equal to zero, then the unit vector t_{ij} of the tangential contact direction is directed along $v_{t,ij}$. If $v_{t,ij}$ is equal to zero, t_{ij} has the same direction as that of the slip. Otherwise t_{ij} is equal to zero, if $v_{t,ij}$ and $\delta_{t,ij}$ are equal to zero, then

$$t_{ij} = \begin{cases} \frac{v_{t,ij}}{|v_{t,ij}|}, v_{t,ij} \neq 0 \\ \frac{\delta_{t,ij}}{|\delta_{t,ij}|}, v_{t,ij}, \delta_{t,ij} \neq 0 \end{cases}$$

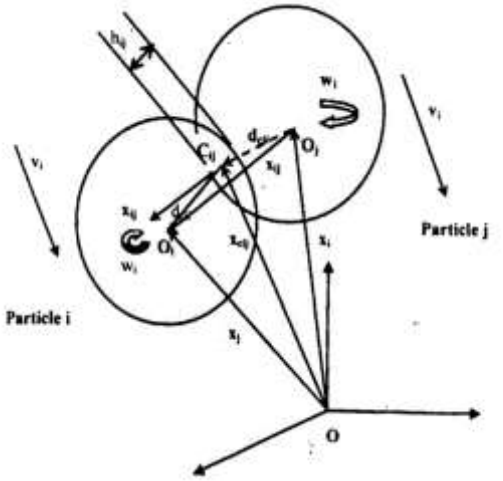

Figure 1: Contact between two particles i and j.

4. Inter Particle Contact Force

The contact force F_{ij} can be expressed as the sum of normal and tangential components;

$$F_{ij} = F_{n,ij} + F_{t,ij}$$

Contact force between the spherical particles are modeled as spring, dash-pots and a friction slider. Spring accounts for elastic repulsion (k).Dash-pot accounts for damping effect η. Friction slider express the tangential friction force in the presence of normal force μ.

The contact forces between them depend on the overlap geometry, the properties of the material and the relative velocity between the particles in the contact area. Hence in the perfect contact model, it is required to describe the effects of elasticity, energy loss through internal friction and surface friction and attraction on the contact surface for describing the contact force calculations.

4.6.1. Normal Force

The normal component of contact force between particles can be expressed as the sum of elastic repulsion, internal friction and the surface attraction forces.

$$F_{n,ij} = F_{n,ij,elastic} + F_{n,ij,viscous}$$

Normal elastic repulsive force is based on the linear Hooke's law of a spring with a spring stiffness constant $K_{n,ij}$ and is given by the expression,

$$F_{n,ij,elastic} = K_{n,ij} h_{ij} n_{ij}$$

Where h_{ij} is the depth of overlap between the contacting particles, n_{ij} is the normal component of the displacement between the particles i and j. The maximum overlap is dependent on the stiffness coefficient.

Normal energy dissipative force is dissipated during real collisions between particles and, in general, it depends on the history of impact. A very simple and popular model is based on the linear dependency of force on the relative velocity of the particles at the contact point with a constant normal dissipation coefficient γ_n and is expressed as

$$F_{n,ij,viscous} = -\gamma_n m_{ij} v_{n,ij}$$

Where γ_n is the normal dissipation coefficient, $v_{n,ij}$ relative normal velocity and m_{ij} is the effective mass of the contacting particle i and j.

$$v_{n,ij} = (v_{ji} \cdot n_{ji}) n_{ji}$$

$$n_{ji} = \begin{cases} 0, x_{ji} = 0 \\ \dfrac{x_{ji}}{|x_{ji}|}, x_{ji \neq 0} \end{cases}$$

$$m_{ij} = \frac{m_i m_j}{m_i + m_j}$$

and x_{ij} is the position from the center of gravity of particle i to that of particle j

$$x_{ij} = x_i - x_j$$

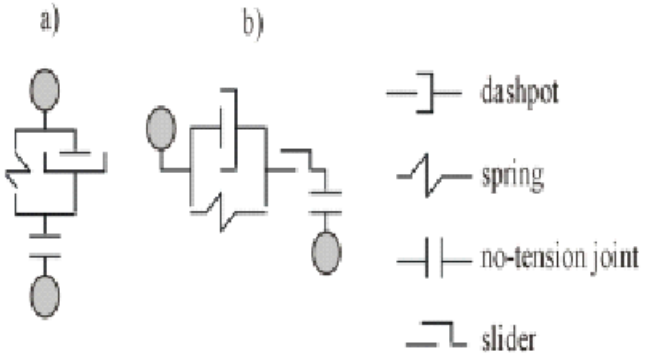

Figure 2: Contact model for DEM simulations in the (a) normal and (b) tangential directions

4.6.2. Tangential force

The tangential component force model depends on the normal force and normal displacement. Further the model for static friction must include energy dissipation, because perpetual oscillations in tangential direction will be obtained during the time of static friction. In the literature two major approaches can be found to represent tangential contact forces namely; global and complex models. Global models describe all the phenomena of the tangential force through a single expression. Complex models describe static and dynamic friction by separate equations and the Coulomb criteria. Of course, the continuous particle interaction models require special models for tangential forces. The tangential force $F_{t,ij}$ being divided into parts of static friction or dynamic friction. When the tangential force $F_{t,ij}$ is larger than the Coulomb-type cut-off limit, dynamic friction predominates. When $F_{t,ij}$ is lower than the limit, the model of static friction force $F_{t,ij,static}$ must be implemented. Such an approach can be modeled by

$$F_{t,ij} = \begin{cases} F_{t,ij,static} \; for \left|F_{t,ij,static}\right| < \left|F_{t,ij} dynamic\right| \\ F_{t,ij,dynamic} \; for \left|F_{t,ij,static}\right| \geq \left|F_{t,ij,dynamic}\right| \end{cases}$$

or Where

$$F_{t,ij} = -t_{ij} \min\left(\left| f_{t,ij,static}\right|, \left| f_{t,ij,dynamic}\right|\right)$$

$F_{t,ij}$ is the unit vector in the tangential direction of the contact point.

Dynamical frictional force can be described as

$F_{t,ij,dynamic} = -\mu \left|F_{n,ij}\right| t_{ij}$, where μ is the dynamic friction coefficient, $F_{n,ij}$ is the normal force and t_{ij} is the unit vector in the tangential direction. Static frictional force is the sum of the tangential spring and energy dissipation force

$F_{t,ij,static} = F_{t,ij,spring} + F_{t,ij,dissipation}$.

Tangential spring force can be described as

$F_{t,ij,spring} = -k_{t,ij} \delta_{t,ij} t_{ij}$

Here, $K_{t,ij}$ is the spring stiffness coefficient and $\delta_{t,ij}$ is the integrated slip in tangential direction after the particles t and j come into contact.

$$\delta_{t,ij} = \left| \int v_{t,ij}(t) dt \right|$$

$$v_{t,ij} = v_{ji} - v_{n,ji}$$

$$v_{n,ji} = \left(v_{ij} \cdot n_{ij}\right) n_{ij}$$

$$v_{ij} = v_{cij} - v_{cji}$$

$$v_{cji} = v_j + \omega_j \times d_{cji}$$

$$v_{cij} = v_i + \omega_i \times d_{cij}$$

$$d_{cij} = -\left(R_i - \frac{h_{ij}}{2}\right) n_{ij}$$

or

$$d_{cij} = x_{cij} - x_i$$

$$d_{cji} = x_{cji} - x_j$$

where $v_{t,ij}$ is the tangential velocity, v_{cij} is the velocity of the contact point of particle i, v_{cji} is the velocity of the contact point of particle j, v_{ij} is the relative velocity of the contact point, v_i is the velocity of particle i, v_j is the velocity of particle j, d_{cij} is the vector directed towards the contact point from the center of particle i, d_{cji} is vector directed towards the contact point from the center of particle j, x_{cij} is the position vector of contact point C_{ij}.

Here $\delta_{t,ij}$ is allowed to increase until the tangential force exceeds the limit imposed by static friction. The vector of tangential displacement $\delta_{t,ij}$ is defined to be perpendicular to the normal contact direction. If tangential velocity $v_{t,ij}$ is not equal to zero, then the unit vector t_{ij} of the tangential contact direction is directed along $v_{t,ij}$. If $v_{t,ij}$ is equal to zero, t_{ij} has the same direction as that of the slip. If t_{ij} is equal to zero, then $v_{t,ij}$ and $\delta_{t,ij}$ are equal to zero.

$$t_{ij} = \begin{cases} \dfrac{v_{t,ij}}{\left|v_{t,ij}\right|}, v_{t,ij} \neq 0 \\ \dfrac{\delta_{t,ij}}{\left|\delta_{t,ij}\right|}, v_{t,ij}, \delta_{t,ij} \neq 0 \end{cases}$$

Friction model for energy dissipation in the tangential direction can be used in the energy dissipation in normal direction

$F_{t,ij,dissipation} = -\gamma_t m_{ij} v_{t,ij}$ Where γ_t is the shear dissipation coefficient, m_{ij} the effective mass of the contacting particles i and j and $v_{t,ij}$ is the tangential velocity. Governing equation for the motion of granular material inside a rotating cylinder.

$$m_i \frac{d^2 x_i}{dt^2} = m_i a_i$$

$$= F_i$$

$$v_i = \frac{dx_i}{dt}$$

Force acting on i^{th} particle F_i is,

$$F_i = m\ g + F_{i,contact}$$

i.e., sum of gravitational force and contact force

$$F_i = m_i g + \sum_{j=i, j\neq i} F_{ij}$$

$$= m_i g + \sum_{\substack{j=i \\ j\neq i}}^{N} \left(F_{n,ij} + F_{t,ij}\right)$$

$$= m_i g + \sum_{\substack{j=i \\ j\neq i}}^{N} F_{n,ij} + \sum_{\substack{j=i \\ j\neq i}}^{N} F_{t,ij}$$

Torque acting on the particle

$$I_i \frac{d^2\theta_i}{dt^2} = T_i$$

$$\omega_i = \frac{d\theta_i}{dt}$$

$$T_i = T_{i,constant}$$

$$= \sum_{\substack{j=i \\ j\neq i}}^{N} T_{ij}$$

$$= \sum_{\substack{j=i \\ j\neq i}}^{N} d_{cij} \times F_{ij}$$

Where d_{cij} is the vector directed towards the contact point from the center of particle i and F_{ij} is the contact force acting between two particles

$$F_{ij} = F_{n,ij} + F_{t,ij}$$

Here F_{ij} shows the contact force exerted by particle j on particle i Particles as contacting viscos-elastic bodies deform each other as depicted in Figure. The contact forces between them depend on the overlap geometry, the material of the particles, and the relative velocity of the particles in the contact area.

5. Boundary Conditions

The properties of granular flow are strongly dependent on the boundary conditions at the wall. Therefore the boundary conditions are very important for an adequate simulation of the granular material behavior. Several types of boundary conditions can be employed:

(a) Walls that may be moving or stationary
(b) Inflow and outflow
(c) Periodic

Walls can be constructed using planes, spheres, cylinders or any other shape as big particles or by an array of small particles. In general, boundaries of the system such as walls are required for the motion of granular material or particles within enclosures, where the wall may have an important influence on the motion of a granular material due to wall-particle interaction. Furthermore, walls can move and rotate around a point of rotation. The rotation of wall particles, in particular is unavoidable in the present study, in which the motion of granular material on the rotating cylinder solely depends on the moving wall. A rotating cylinder can be constructed by a cylinder or sphere with a negative radius. Collisions between particles and walls are defined by the material and geometry of the particles and walls, as in the case of collisions between particles. It is convenient to construct rough walls by an array of particles (Thompson and Grest[1991]). For the present formulation the following methodology is adapted; the system under consideration has been modelled by an ensemble of spheres possessing the same material constants as that of the grains inside the container. The motion of the wall spheres is not affected by the impacts but is, strictly governed by the continuous rotation of the cylinder. The calculation of contact forces between the particles and wall are defined in the same way as between particles.

6. The Surrounding Media

The effect of surrounding media or physical field acting on the particle may be added as additional forces. In the current approach the effect of gravity field is taken into account.

7. Numerical Model

In the present study DEM is used to simulate the dynamic behavior of granular materials in a rotating drum (calciner).Granular material is considered here as a collection of frictional elastic spherical particles. The equations of motion for each particle are derived from Newton's law of classical Newtonian dynamics. These include a system of equations for the translational motion of centre of gravity and rotational motion around the centre of gravity for each particle in the granular medium. Translational motion of the centre of gravity of a particle i can be fully described by a system of equations (Algis Dzingys [2001]).

$$m_i \frac{d^2x_i}{dt^2} = m_i a_i = F_i$$

Rotational motion of the particle i around the centre of gravity can be fully described by the following systems of equations (Algis Dzingys [2001]).

$$I_i \frac{d^2\theta_i}{dt^2} = T_i$$

Each particle may interact with its neighbors or with the boundary only at contact points through normal and tangential forces. The forces and torques acting on each of the particles are calculated as

$$F_i = F_{i,contact} + F_{i,gravity} + F_{i,external}$$

$$T_i = T_{i,contact} + T_{i,fluid} + T_{i,external}$$

Thus, the force on each particle is given by the sum of gravitational, inter-particle (normal force and tangential force) and external forces). The corresponding torque on each particle is the sum of the total torque caused by anti-symmetric fluid drag forces, the summation of torques caused by other external forces and the summation of all the torques caused by the contact forces between the particles. The normal forces are calculated using the "spring dashpot model"), which allows colliding particles to overlap slightly. The normal interaction force is a function of the overlap.
The contact force F_{ij} can be expressed as the sum of normal and tangential components;

$$F_{ij} = F_{n,ij} + F_{t,ij}$$

Contact force between the spherical particles are modelled as spring, dash-pots and a friction slider. Spring accounts for elastic repulsion (k).Dash-pot accounts for damping effect (η). Friction slider express the tangential friction force in the presence of normal force (μ).

The contact forces between particles depend on the overlap geometry, the properties of the material and the relative velocity between the particles in the contact area. Hence in the perfect contact model, it is required to describe the effects of elasticity, energy loss through internal friction and surface friction and attraction on the contact surface for describing the contact force calculations.

The normal component of contact force between particles can be expressed as the sum of elastic repulsion, internal friction and the surface attraction forces.

$$F_{n,ij} = F_{n,ij,elastic} + F_{n,ij,viscous}$$

8. Time Integration Scheme

Various time integration schemes can be used to solve the equations. The main requirements for a good scheme are given below:

- It should be stable
- It should satisfy the required accuracy
- It preferably should satisfy energy and momentum conservation
- It should not require excessive memory

Time consuming calculation of inter-particle forces should be carried to the minimum possible extent-ideally, once per time step, Δt

Some of the most popular schemes used in DEM by various authors include; first order Euler's scheme, Fourth-order Runge Kutta method (Ovensen et al., [1996], AlIen and Tildseley, (1987], Shida et al., [1997]), velocity verlet scheme (Aoki and Akiyama [1995], Kopf et al., [1997], Satoh [1995a, 1995bD, second order AdamsBashforth scheme (Sundaram and Collins [1996]) and predictor-corrector schemes (Newmark and Asce, [1959]), Thompson and Grest [1991], Form et al. [1993], Lee
And Hermann [1993]).

Van Gunsteren and Berendsen [1977J compared the Gear predictor-corrector, Runge-Kutta and verlet schemes for macromolecular simulations and concluded that Gear scheme is the best for small time steps and verlet algorithm for larger time steps.

Hence the 5th order Gear predictor-corrector scheme (Alien and Tildseley, 1987) is used in this work to solve the equations, which is stable for second-order differential equations with global truncation error of

$$O\left(\Delta t^{q+1-2}\right) = O\left(\Delta t^{q-1}\right)$$

$$x_i(t+\Delta t) = x_i(t) + \dot{x}(t)\Delta t + \ddot{x}_i(t)\frac{(\Delta t)^2}{2!} + \dddot{x}(t)\frac{(\Delta t)^3}{3!} + x_i^{(iv)}(t)\frac{(\Delta t)^4}{4!} + x_i^{(v)}(t)\frac{(\Delta t)^5}{5!}$$

$$\dot{x}_i(t+\Delta t) = \dot{x}_i(t) + \ddot{x}_i(t)\Delta t + \dddot{x}(t)\frac{(\Delta t)^2}{2!} + x_i^{(iv)}(t)\frac{(\Delta t)^3}{3!} + x_i^{(v)}(t)\frac{(\Delta t)^4}{4!}$$

$$\ddot{x}_i(t+\Delta t) = \ddot{x}_i(t) + \dddot{x}_i(t)\Delta t + x_i^{(iv)}(t)\frac{(\Delta t)^2}{2!} + x_i^{(v)}(t)\frac{(\Delta t)^3}{3!}$$

$$\dddot{x}_i(t+\Delta t) = \dddot{x}_i(t) + x_i^{(iv)}(t)\Delta t + x_i^{(v)}(t)\frac{(\Delta t)^2}{2!}$$

$$x_i^{(iv)}(t+\Delta t) = x_i^{(iv)}(t) + x_i^{(v)}(t)\Delta t$$

$$x_i^{(v)}(t+\Delta t) = x_i^{(v)}(t)$$

Then the inter particle forces acting on each particle at time $(t+\Delta t)$is evaluated using the predicted particle positions. Applying the obtained evaluated forces at time $(t+\Delta t)$ and Newton's second law, the particle accelerations $\ddot{x}(t+\Delta t)$ can be determined. The difference between the predicted accelerations and evaluated accelerations is then computed;

$$\Delta \ddot{x}_i = \ddot{x}_i(t+\Delta t) - \ddot{x}_i^{p}(t+\Delta t)$$

The predicted particle positions and their derivatives are corrected using the difference, $\Delta \ddot{x}$, obtained between the predicted accelerations and that given by the evaluated force.
In the Gear's Predictor Corrector algorithm, this difference term is used to correct all the predicted t particle positions and their derivatives. The correction terms are given by;

$$x_i = x_i^{p} + \alpha_0 \Delta R_2$$

$$\dot{x}_i \Delta t = \dot{x}_i^{p} \Delta t + \alpha_1 \Delta R_2$$

$$\frac{\ddot{x}_i(\Delta t)^2}{2!} = \frac{\ddot{x}_i^{p}(\Delta t)^2}{2!} + \alpha_2 \Delta R_2$$

$$\frac{\dddot{x}_i(\Delta t)^3}{3!} = \frac{\dddot{x}_i^{p}(\Delta t)^3}{3!} + \alpha_3 \Delta R_2$$

$$\frac{x_i^{(iv)}(\Delta t)^4}{4!} = \frac{x_i^{(iv)p}(\Delta t)^4}{4!} + \alpha_4 \Delta R_2$$

$$\frac{x_i^{(v)}(\Delta t)^5}{5!} = \frac{x_i^{(v)p}(\Delta t)^5}{5!} + \alpha_5 \Delta R_2$$

Where,

$$\Delta R_2 = \frac{\Delta \ddot{x}_i (\Delta t)^2}{2!}$$

Values of parameters α_i (Alien and Tildseley, [1987]) for second order differential equations of predicting order q are presented in table 3.1.

Table 3.1: Values of the parameter a,

α_i	q=3	q=4	q=5
α_1	$\frac{1}{6}$	$\frac{19}{12}$	$\frac{3}{16}$
α_2	$\frac{5}{6}$	$\frac{3}{4}$	$\frac{251}{360}$
α_3	1	1	1
α_4	$\frac{1}{3}$	$\frac{1}{2}$	$\frac{11}{18}$
α_5	-	$\frac{1}{12}$	$\frac{1}{6}$
α_6	-	-	$\frac{1}{60}$

The parameter, α_i promotes numerical stability of the algorithm. The solution of equations (3.33) to (3.36) was carried out by a 5th order Gear Predictor-Corrector scheme (AlIen and Tildseley, [1987]). The time step Δt of thex integration was chosen such that the entire contact between the particles was resolved within 10 time steps at least.

The time step Δt, for the time integration of the particle position, velocity, orientation and angular velocity depends on the time of contact T_c, which can be expressed as

$$T_c = \lambda \sqrt{\frac{m}{k}}$$

Which is estimated based on the single degree of freedom system of mass m connected to the ground by a spring of stiffness k. Hence the time step must be sufficiently small to ensure a stable numerical scheme of time integration and Cundall and Strack [1979] proposed that the time step must be smaller than the critical time step

$$\Delta T_c = \sqrt{\frac{m}{k}}$$

9. Computer Implementation

The major computational tasks of DEM at each time step can be summarized as follows:

- Finding the neighbour list for each particle
- Detection of contacts between a particle i and its neighbours
- Computation of contact forces from relative displacement between particles
- Summation of contact forces to determine the total unbalanced force
- Computation of acceleration from force
- Velocity and displacement by integrating the acceleration
- Updating the position of particles

10. Granular Bed Motion in the Transverse Plane

The motion of a bed of granular solids in the transverse plane of a rotated cylinder can take different forms, as described by (Henein et al. [1983 a]). As the cylinder rotation speed is increased from zero, six distinct modes of bed behavior viz., slipping, slumping, rolling, cascading, cataracting and centrifuging are observed, as shown schematically in Figure 2.

10.1 Slipping Mode

At very low rotational speeds, particularly when the friction between the granular bed and the cylinder wall is low, the granular bed performs as a rigid body. The bed motion is observed to take one of two forms (i) the granular bed remains at rest and the granular solid continuously slides at the wall, or (ii) the granular solid repeatedly moves upward with the cylinder until the bed surface reaches a maximum inclination and then slips at the wall back to a minimum inclination and then resumes rotation.

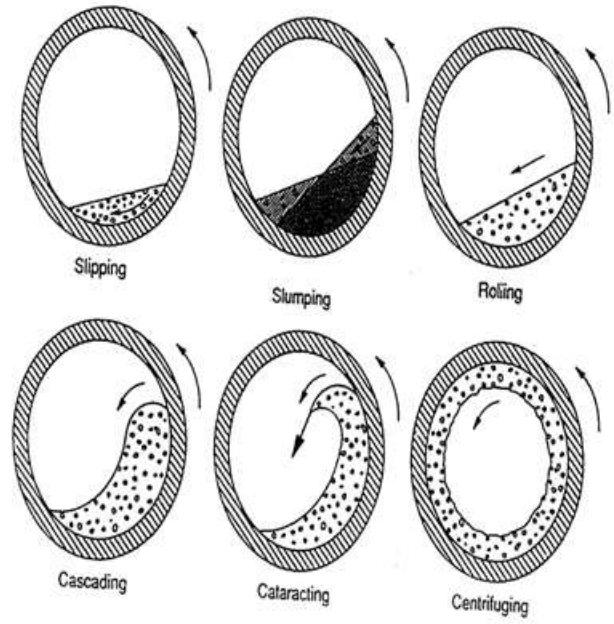

Figure 2: Schematic view of the different modes of solids motion (Boateng, [1993])

10.2 Slumping Mode

In this mode, the granular solid is raised like a rigid body by the cylinder wall such that the feeling of the bed surface

increases unceasingly until it reaches an upper angle of repose then separates from the upper surface of the bed, and falls as a discrete avalanche toward the lower half of the bed. Next the avalanche the inclination of the surface of the granular solid drops to an angle of repose that is less than the static angle of repose of the granular solid. The slumping frequency is experiential to increase with increasing rotation speed, finally leading to the rolling mode. The change between the slumping and rolling modes of bed motion is not always obviously defined, rather the bed behaviour is found to go through a transition in which the bed changes randomly between rolling and slumping behaviour.

10.3. Rolling Mode

The majority of the bed rotates as a rigid body about the cylinder axis at the same rotation speed as the cylinder wall. On the bed surface there appears a thin layer of continuously falling particles forming a plane free surface that is inclined at the dynamic angle of repose of the granular solid to the horizontal plane. Solid particles mix more effectively in the rolling mode. In the rolling mode, bed material can be divided into two distinct regions, namely a 'passive region or plug flow region' where the particles are carried upward by the cylinder wall, and a relatively thin 'active region or cascading layers. In the passive region, granular mixing is negligible and the mixing mainly occurs in the active region. At higher mixer rotational speeds, the continuous flow rolling regime is obtained, in which a thin layer of particles flows down the free surface while the remaining particles rotate as a fixed bed. Transverse mixing in this event depends on the dynamics and outcomes from the shearing and collisional diffusion inside the layer.

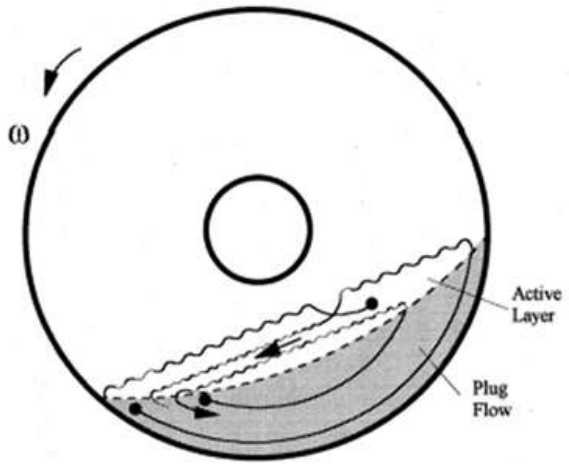

Figure 3: Rolling bed motion: top plane- active (shear) layer; bottom plane –plug flow (non-shearing region), (Boateng [1993])

10.4. Cascading Mode

As the rotation speed is increased additional, the particles in the upper corner of the rolling bed are lifted higher before detaching from the cylinder wall, and the bed surface assumes a crescent shape in the cylinder cross-section. This mode of material motion is termed as cascading mode.

10.5. Cataracting Mode

On further increasing the rotational speed, centrifugal forces become increasingly significant in the motion of particles along the bed surface, the curvature of the cascading surface becomes highly pronounced and particles are projected into the freeboard space from the upper corner of the bed.

10.6. Centrifuging Mode

At a Froude number of unity, the granular solid is restrained to the inner wall of the cylinder by centrifugal forces. According to [Nityanand et at. 1986], the critical rotational speed at which a particle at the cylinder wall starts centrifuging can be calculated from the equation where g is the acceleration due to gravity and 0 is the diameter of the cylinder.

11. Simulation conditions and procedures

11.1. Initial Condition.

The transverse plane of a horizontal cylinder is a circle. This is represented as a set of spherical particles at a distance equal to the cylinder radius from the origin of the Cartesian coordinate system chosen. The origin of the coordinate system is at the center of the circle as shown in Figure 4.1.

The initial condition, r=0 of granular solids in the transverse plane of the rotating cylinder is assumed to be a packed bed of granular solids. Since the initial conditions of granular particles in a packed bed cannot be specified a priori. The calculations were carried out at two stages. Given the fill fraction, particle sizes and their distribution, the number of particles for each size range was determined using equation

$$np(i) = \frac{4\, fw_i A}{\lambda d_p(i)^2}$$

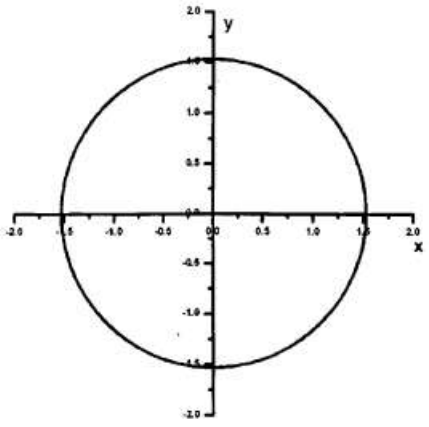

Figure 4: Coordinate system chosen for simulation.

Where fw_i is the percentage of fraction of the particles of size $d_p(i)^2$ and A is the cross sectional area of the bed. An orthogonal grid is then generated with the size of the grid equal to the diameter of the largest particle and the particles are placed at the center of these grids so that they don't

overlap over each other. Uniform sized particles are given a particular colour. Figure 4.2 shows one such initial distribution generated for two different sized particles at equal number concentrations.

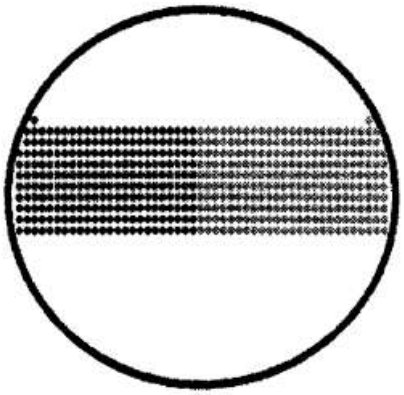

Figure 5: Initial Distribution of the particles

The initial velocities of individual particles were chosen randomly and the force of gravity is allowed to act on each particle.

11.2. Force due to gravity

Initially the particles fall under gravity since there is no contact force, but after some time the contact forces also come into play. The bordering shape of the rotating cylinder, which first stops the pure vertical motion and secondly causes the particles to interact with each other, limits the motion of the particles. The total kinetic energy of the system is calculated as follows;

$$KE = \frac{1}{2}\sum_{i=1}^{N_p} m_i v_i^2$$

Where mi is the mass, V_i is the velocity and N_p is the total number of particles in the system The simulation was continued till all the particles came to rest; that is until the total kinetic energy of the system becomes negligible as shown in Figures 4.3 (a) and (b). The location and linear and rotational velocities of particles at this stage are chosen as the initial conditions for the next stage of simulation.

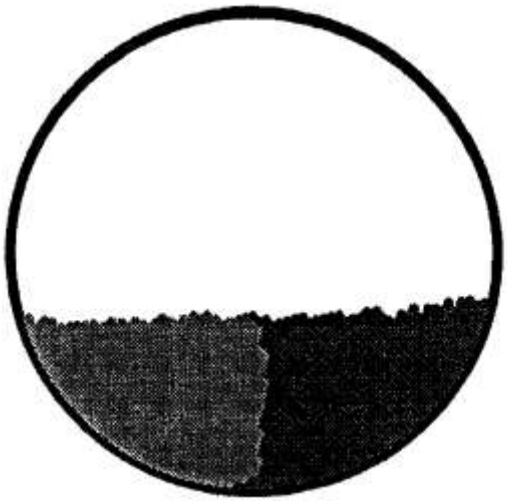

Figure 4.3: Initial packed bed

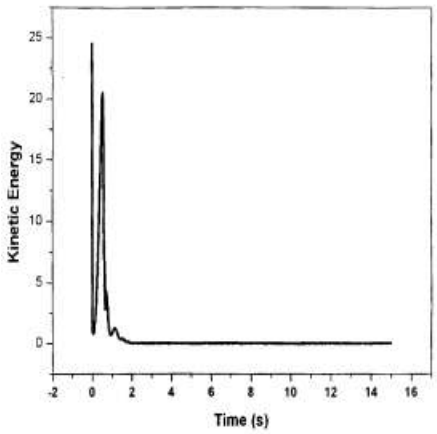

Figure 4.4: Total kinetic energy with respect to time

12. Conclusion

The result obtained in the present investigation may be generally described as follows:

1. The described discrete element model composed of visco-elastic spherical particles is implemented into the developed C++ code. This code open for new elements and interaction models may be considered as the first step in the development of an advanced simulation tool for granular and other inhomogeneous materials and is intended for modelling more complex geotechnical problems.
2. The time integration tests conducted with particle-particle and particle-wall interaction have proved that the performance of 5th order Gear predictor corrector scheme is the better compared to the integration methods. This scheme is implemented into the code.

Reference

[1] Algis Dzingys and Bernhard Peters, "An approach to simulate the motion of spherical and non-spherical fuel particles in combustion chambers", Granular. Matter 3, 231 (2001).
[2] Algis Dzingys and Bernhard Peters, "An approach to simulate the motion of spherical and non-spherical fuel particles in combustion chambers", Granular. Matter 3, 231 (2001).
[3] Allen M. P. and Tildseley D. F., Computer Simulation of Liquids, Clarenden Press, Oxford, 1987
[4] Bodhisattwa Chaudhuri, Fernando J. Muzzio, M. Silvina Tomassone .Modeling of heat transfer in granular flow in rotating vessels. Chemical Engineering Science 61 (2006) 6348 – 6360
[5] Cleary, P. W.; Sawley, M.L.DEM modelling of industrial granular flows: 3D case studies and the effect of particle shape on hopper discharge. Applied Mathematical Modeling, 26, 2002, P. 89-111.
[6] Cundall P. A. and O. D. L. Strack, "A discrete numerical model for granular assemblies", Geotechnique 29, 47 (1979).
[7] Cundall, P.A., 1971. A computer model for simulating progressive large scale movements in blocky rock

systems. Proceedings of Symposium International Society of Rock Mechanics 2, 129.
[8] Dippel, S., Batrouni, G.G., Wolf, D.E., 1996. Collision-induced friction in the motion of a single particle on a bumpy inclined line. Physical Review E 54, 6845.
[9] E.N. Zeigler, S. Agarwal, on the optimum heat transfer coefficient at an exchange surface in a gas fluidized bed, Chemical Engineering Science 24 (1969) 1235
[10] Figueroa I, Vargas WL, McCarthy JJ. Mixing and heat conduction in rotating tumblers. Chem Eng Sci. 2010; 65:1045–1054.
[11] Figueroa, I.; Vargas, W.L.; McCarthy, J.J. 2010. Mixing and heat conduction in rotating tumblers, Chemical Engineering Science 65: 1045-1054.
[12] Henein, H., Brimacombe, J.K., Watkinson, A.P. Experimental studies of transverse bed motion in rotary kilns. Metall. Trans. B. 14B, 191–205 (1983).
[13] Kantor, A. L.; Long,L. N.; Micci, M. M. Molecular dynamics simulation of dissotiantion kinetics. In: AIAA Aersospace Science Meeting, AIAA Paper 2000-0213,2000
[14] Kuwagia,K.; Horio, M. A numerical study on agglomerate formation in a fluidized bed of fine cohesive particles. Chemical Engineering Science, 57, 2002, p. 4737-4744.
[15] Lehmberg J., M. Hehl and K. Schugerl, "Transverse mixing and heat transfer in horizontal rotary drum reactors", Powder. Technol. 18, 149 (1977).
[16] Li, J.T. & Mason, D.J. (2000). A computational investigation of transient heat transfer in pneumatic transport of granular particles. Powder Technol., 112, 273-282, 0032-5910.
[17] Luding, S., 1997. Stress distribution in static two dimensional granular model media in the absence of friction. Physical Review E 55, 4720.
[18] Moakher, M., Shinbrot, T., Muzzio, F.J., 2000. Experimentally validated computations of flow, mixing and segregation of non-cohesive grains in 3D tumbling blenders. Powder Technology 109, 58.
[19] Nguyen, V.D., Cogne, C., Guessasma, M., Bellenger, E., Fortin, J., 2009. Discrete modeling of granular flow with thermal transfer: application to the discharge of silos. Appl. Therm. Eng. 29, 1846e1853
[20] Nityanand N., B. Manley and H. Henein, "An analysis of radial segregation for different sized spherical solids in rotary cylinders", Met. Tram. B 178, 247 (1986).
[21] O.O. Ajayi, M.E. Sheehan, Design loading of free flowing and cohesive solids in flighted rotary dryers, Chem. Eng. Sci. 73 (2012) 400–411.
[22] P. Shao, K. Darcovich, T. McCracken, G. Ordorica-Garcia, M. Reith, S. O'Leary, Algaede watering using rotary drum vacuum filters: process modeling, simulation andtechno-economics, Chem. Eng. J. 268 (2015) 67–75
[23] Perry, H.R., Chilton, C.H. (1984). Chemical Engineers' Handbook, vol. 6.McGraw-Hill, New York, pp. 11–46.
[24] R. Schmidt, P. a. Nikrityuk, Numerical simulation of the transient temperature distribution in side moving particles, Can. J. Chem. Eng. 90 (2012) 246–262.
[25] Ristow, G.H., 1996. Dynamics of granular material in a rotating drum. Euro physics Letters 34, 263.
[26] Ristow, G.H., Herrmann, H.J., 1994. Density patterns in two-dimensional hoppers. Physical Review E 50, R5.
[27] Shinbrot, T., Alexander, A., Moakher, M., Muzzio, F.J., 1999. Chaotic granular mixing. Chaos 9, 611.
[28] Tanaka, K.; Nishida, M.; Kunimochi, T.; Takagi, T. Discrete element simulation and experiment for dynamic response of two-dimensional granular matter to the impact of a spherical projectile. Powder Technology, 124, 2002, p. 160-173.
[29] Thompson, P.S., Grest, G.S., 1991. Granular flow: friction and the dilatancy transition. Physical Review Letters 67, 1751.
[30] Tran, T. X.; Dorfman, A.; Rhie, Y.B. Micromechanical modeling of cracking and damage of concrete. In: Computational Modeling of Concrete Structures, Rotterdam. Balkema, 1998, P. 61-69.
[31] Wightman, C., Moakher, M., Muzzio, F.J., Walton, O.R., 1998. Simulation of flow and mixing of particles in a rotating and rocking cylinder. A.I.Ch.E. Journal 44, 1226.